Acta Mech 226, 1341–1357 (2015)
DOI 10.1007/s00707-014-1252-8

Xufeng Yang · Yongshou Liu · Yishang Zhang · Zhufeng Yue

Hybrid reliability analysis with both random and probability-box variables

Received: 10 March 2014 / Revised: 25 July 2014 / Published online: 18 December 2014
© Springer-Verlag Wien 2014

Abstract Hybrid reliability analysis (HRA) with both aleatory and epistemic uncertainties is investigated in this paper. The aleatory uncertainties are described by random variables, and the epistemic uncertainties are described by a probability-box (*p*-box) model. Although tremendous efforts have been devoted to propagating random or *p*-box uncertainties, much less attention has been paid to analyzing the hybrid reliability with both of them. For HRA, optimization-based Interval Monte Carlo Simulation (OIMCS) is available to estimate the bounds of failure probability, but it requires enormous computational performance. A new method combining the Kriging model with OIMCS is proposed in this paper. When constructing the Kriging model, we only locally approximate the performance function in the region where the sign is prone to be wrongly predicted. It is based on the idea that a surrogate model only exactly predicting the sign of performance function could satisfy the demand of accuracy for HRA. Then OIMCS can be effectively performed based on the Kriging model. Three numerical examples and an engineering application are investigated to demonstrate the performance of the proposed method.

1 Introduction

Uncertainties with respect to loading, material properties, manufacturing imprecision, imperfect knowledge, etc., are ubiquitous in practical engineering problems. They significantly affect the performance and safety of a product. Quantification of such uncertainties and the corresponding reliability analysis is an essential task throughout the life cycle of a product.

Generally speaking, uncertainties can be classified into two distinct types: aleatory ones and epistemic ones [1,2]. Aleatory uncertainty is also referred to as objective uncertainty, which results from natural variability and is irreducible. They are usually described by a probabilistic model, and the classical probability theory is widely utilized to propagate the aleatory uncertainties. Epistemic uncertainty is a subjective and reducible uncertainty that arises from lack of knowledge or data. Different kinds of theories have been elaborated to tackle epistemic uncertainties, which include Bayesian approaches [3,4], interval probabilities [5,6], probability boxes (*p*-box for short) [7,8], evidence theory [2,9], fuzzy sets [10,11], info-gap theory [12,13], and so forth.

Classical probability theory requires precise probability distributions of the uncertainties, which may be impossible for some variables due to limited experimental data. In this case, unwarranted assumptions in constructing a probabilistic model may result in misleading results [14]. Without precise probabilistic models,

X. Yang · Y. Liu (✉) · Y. Zhang · Z. Yue
Department of Engineering Mechanics, Institute of Aircraft Reliability Engineering Northwestern Polytechnical University, Xi'an 710072, People's Republic of China
E-mail: yongshouliu@nwpu.edu.cn

X. Yang
E-mail: xufengyang0322@gmail.com

it is suitable to treat the uncertain parameters as epistemic uncertainties. In this article, p-box is adopted to describe an uncertain variable without precise probabilistic distribution. A p-box is a pair of lower and upper cumulative distribution functions (CDFs) [7]. In the theory of p-box, the CDF of an uncertain variable is assumed to be bounded in a p-box. This bounding approach permits analysts to carry out reliability analysis without requiring overly precise assumptions about the values of distribution parameters or distribution shapes [15]. Therefore, it has attracted much attention in the field of reliability analysis, and diverse approaches have been proposed during the past several years.

The task of reliability analysis with uncertainties modeled by p-boxes is to estimate the bounds of failure probability. Routinely, the Cartesian product method (CPM) [16] was used to fulfill this task. Inspired by the sampling technique in Refs. [17–19], Zhang et al. proposed an interval Monte Carlo Simulation (IMCS) method [20], an interval importance sampling method [21] and an interval quasi-MCS method [22]. Jiang et al. [23] proposed a numerical method based on first-order reliability method. Hurtado [24] developed a brand new method based on the technique of reliability plot. Other techniques to propagate p-box uncertainties in structural systems can also be found in Refs. [25,26].

In many engineering applications, a frequently confronted case is that some of the uncertainties can be quantified with certain probability distributions and others have to be treated as epistemic variables [27,28]. Hybrid reliability analysis (HRA) with both aleatory and epistemic variables has attracted much attention in such circumstances. In this field, probability theory has been well integrated with the info-gap theory [28,29], the evidence theory [30,31] and fuzzy sets theory [32]. However, few researchers have considered the condition with both random variables and p-box variables.

This paper aims to develop an efficient and accurate method for HRA with both random variables and p-box variables. When both random variables and epistemic variables modeled with p-box model present in an uncertain structure, IMCS is applicable to analyze the reliability. In IMCS, the extrema of structural performance function entail to be obtained and interval arithmetic is adopted to fulfill this task. However, interval arithmetic is not applicable to black-box functions [33]. Optimization strategy is competent to search the extrema of a black-box function [33,34]. Nevertheless, this entails enormous calls to the true performance function. For a practical engineering structure whose performance function needs to be obtained by time-consuming finite element (FE) analysis, optimization-based IMCS (OIMCS) will become impossible for enormous calls to the FE codes.

So, a surrogate model is introduced to approximate the performance function in this paper. It is figured out that a surrogate model only exactly predicting the sign of performance function rather than its specific value can satisfy the requirement of accuracy for HRA. Then, we propose an active learning Kriging (ALK) model only finely approximating the sign of the performance function. Based on the Kriging model, the extrema of the performance function are searched by optimization strategy at each simulated sample and OIMCS is effectively implemented to estimate the bounds of failure probability. The proposed method is called ALK-OIMCS in this paper. ALK-OIMCS avoids the utilization of interval arithmetic, so it is competent to tackle a problem with black-box performance function. In addition, the presented method is accurate enough with evaluating the performance function as few times as possible because of its local approximation.

The rest of this paper is organized as follows. In Sect. 2, the theory of HRA with both random and p-box variables is described. OIMCS method is presented in Sect. 3 which will be the benchmark of the suggested method. Section 4 addresses the proposed ALK-OIMCS methodology. Four case studies are presented to demonstrate the effectiveness of the suggested method in Sect. 5. Conclusions are made in the last section.

2 Hybrid reliability analysis with both random and p-box variables

2.1 Preliminaries of p-box

In the p-box theory, the CDF of an uncertain variable is assumed to be bounded in a pair of lower and upper CDFs. For an epistemic variable P with a realization p, denote its CDF as $F_P(p)$. Nothing is known about its CDF except that it satisfies the inequalities as

$$\underline{F}_P(p) \le F_P(p) \le \overline{F}_P(p). \tag{1}$$

The lower CDF $\underline{F}_P(p)$ and the upper CDF $\overline{F}_P(p)$ define a "p-box". Various ways have been suggested to construct a p-box, including the Kolmogorov–Smirnov confidence limits, Chebyshev's inequality, distributions with interval parameters, and the envelope of competing probabilistic models [8,22]. According to the amount

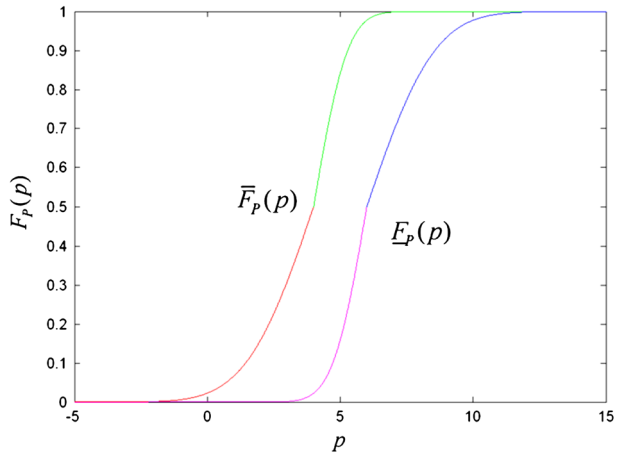

Fig. 1 p-Box of a normal distributed variable with interval parameters

of available information, analysts may choose among them. This paper focuses on the kind of p-box constructed by distributions with interval parameters.

Based on the observational data, a confidence interval can be obtained with classical statistical approaches. Consequentially, the (unknown) distribution parameter of a variable is located within an interval at a specified level of confidence [22]. Thus, distribution with interval parameters provides a natural way to define a p-box. Take a normal distributed variable P for example, whose mean value and standard deviation, respectively, are located in the intervals [4, 6] and [1, 2]. The CDF of P is bounded in a p-box, as shown in Fig. 1.

2.2 Hybrid reliability analysis

When only random variables exist in an uncertain structure, the reliability can be analyzed by traditional Monte Carlo Simulation method. The performance function is denoted as

$$G(\mathbf{X}) = b - g(\mathbf{X}), \tag{2}$$

where b is a suitable threshold, $\mathbf{X} = \left[X_1, X_2 \ldots X_{n_X}\right]$ is the vector of random variables and $g(\cdot)$ is the structural response. The failure probability P_f is defined by

$$P_f = \mathrm{P}\left\{G(\mathbf{X}) < 0\right\} = \underset{G(\mathbf{x})<0}{\iint \cdots \int} f_{\mathbf{X}}(\mathbf{x})\mathrm{d}\mathbf{x}, \tag{3}$$

where $f_{\mathbf{X}}(\cdot)$ is the joint probability density function (PDF) of $\mathbf{X}$, $\mathbf{x}$ is a realization of $\mathbf{X}$. Equation (3) can be rewritten as

$$\begin{aligned} P_f &= \iint \cdots \int I_F(\mathbf{x}) f(\mathbf{x})\mathrm{d}\mathbf{x} \\ &= \frac{1}{N}\sum_{j=1}^{N} I_F\left[G(\mathbf{x}^{(j)}) < 0\right], \end{aligned} \tag{4}$$

where $\mathbf{x}^{(j)}$ is the jth simulated sample of random variables. N is the number of samples. $I_F(\cdot)$ is the failure indicator function with the value 1 if $\cdot$ is "true" and the value 0 if $\cdot$ is "false".

Generally, the simulated samples are generated with the inverse transform method [35], that is

$$\mathbf{x}^{(j)} = F_{\mathbf{X}}^{-1}(\mathbf{r}^{(j)}), \quad j = 1, 2, \ldots, N, \tag{5}$$

in which $\mathbf{r}^{(j)}$ is the jth standard uniform sample.

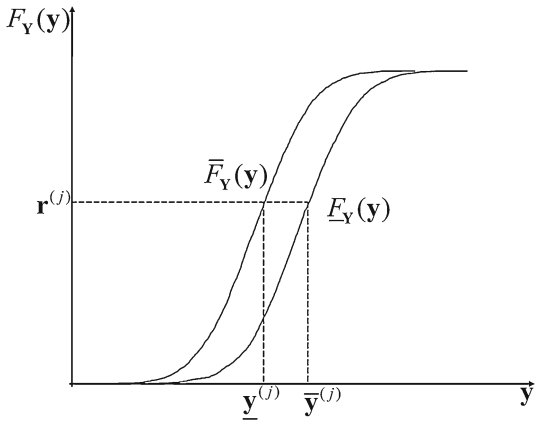

Fig. 2 Inverse transform of a p-box variable

When epistemic uncertainties are also present, the performance function is expressed as

$$G(\mathbf{X}, \mathbf{Y}) = b - g(\mathbf{X}, \mathbf{Y}), \tag{6}$$

where $\mathbf{Y} = \left[Y_1, Y_2, \ldots, Y_{n_Y}\right]$ is the vector of epistemic variables characterized with the p-box model. The realization of $\mathbf{Y}$ is denoted as $\mathbf{y}$. The CDF of p-box variables $F_{\mathbf{Y}}(\cdot)$ is not a determinate function, but an interval function. Then, the simulated samples obtained with the inverse transform method are not determinate random numbers but intervals, as shown in Fig. 2. Denote $\overline{\mathbf{y}}^{(j)}$ and $\underline{\mathbf{y}}^{(j)}$ as the lower bound and upper bounds of the jth interval sample, and

$$\overline{\mathbf{y}}^{(j)} = \underline{F}_{\mathbf{Y}}^{-1}\left(\mathbf{r}^{(j)}\right), \tag{7}$$

$$\underline{\mathbf{y}}^{(j)} = \overline{F}_{\mathbf{Y}}^{-1}\left(\mathbf{r}^{(j)}\right). \tag{8}$$

At the jth simulated sample, $\mathbf{x}^{(j)}$ is a determinate value while $\mathbf{y}^{(j)}$ is an interval. Then, the performance function at each sample is also an interval, so is the failure probability. The lower bound and upper bound of the performance function at each simulated sample are, respectively, obtained by

$$\underline{G}^{(j)} = \min_{\mathbf{y}\in\mathbf{C}_j} G\left(\mathbf{x}^{(j)}, \mathbf{y}\right) \tag{9}$$

and

$$\overline{G}^{(j)} = \max_{\mathbf{y}\in\mathbf{C}_j} G\left(\mathbf{x}^{(j)}, \mathbf{y}\right), \tag{10}$$

where $\mathbf{C}_j$ is the jth interval space defined by $\mathbf{C}_j = \left[\underline{\mathbf{y}}^{(j)}, \overline{\mathbf{y}}^{(j)}\right]$. The lower and upper bounds of failure probability are, respectively, given by

$$\underline{P}_f = \frac{1}{N}\sum_{j=1}^{N} I_F\left(\overline{G}^{(j)} < 0\right) \tag{11}$$

and

$$\overline{P}_f = \frac{1}{N}\sum_{j=1}^{N} I_F\left(\underline{G}^{(j)} < 0\right). \tag{12}$$

3 Optimization-based interval Monte Carlo simulation (OIMCS)

Then, the OIMCS can be employed to estimate the bounds of failure probability through the following four steps:

1. Generate N samples uniformly distributed between 0 and 1.
   Both the random sampling method (RSM) and low-discrepancy sampling method (LSM) are available to generate these samples. Considering that the samples in LSM are more uniformly distributed than the ones in RSM [22,36], LSM is adopted and the Hammersley sequence [37] is utilized in this paper.
2. Obtain the simulated samples transformed from the uniform samples with Eqs. (5), (7) and (8).
3. For the jth simulated sample, compute the extrema of $G(\mathbf{x}, \mathbf{y})$ with Eqs. (9) and (10).
   The optimization method, sampling method, vertex method and interval arithmetic are available to obtain the extrema [11]. The optimization method does not greatly suffer the curse of dimensionality and is not restricted by the non-monotony or the implicitness of the performance function [11]. Therefore, the optimization method is employed. To find the global optimal solution, a global optimization technique is required and the DIRECT algorithm [38] is adopted in this paper.
4. Obtain the signs of extrema and compute the bounds of failure probability with Eqs. (11) and (12).

4 ALK-OIMCS

4.1 Basic idea

OIMCS is a nested procedure with sampling and optimization which entails enormous calls to the true performance function. For a practical engineering problem, the performance function usually needs to be computed with time-consuming FE analysis or computational fluid dynamics. Then, it will be very tricky to obtain the bounds of failure probability with OIMCS. So, it is feasible to introduce a Kriging model to approximate the performance function and then compute $\overline{P}_f$ and $\underline{P}_f$ with OIMCS based on the Kriging model.

ALK-OIMCS is aimed at rightly predicting the sign of $G(\mathbf{x}, \mathbf{y})$ rather than its specific value. That is, the Kriging model does not approximate $G(\mathbf{x}, \mathbf{y})$ throughout the uncertain space, but only in the region of interest. So, we can carry out HRA with calling the performance function as few times as possible. The main idea of ALK-OIMCS is that a Kriging model only able to rightly predict the sign of $G(\mathbf{x}, \mathbf{y})$ can meet the accuracy required for HRA. The following is the reason:

Property 1 *If a Kriging model* $\hat{G}(\mathbf{x}, \mathbf{y})$ *can rightly predict the sign of* $G(\mathbf{x}, \mathbf{y})$*, then the sign of* $\min_{\mathbf{y}\in\mathbf{C}_j} G\left(\mathbf{x}^{(j)}, \mathbf{y}\right)$ *is the same as that of* $\min_{\mathbf{y}\in\mathbf{C}_j} \hat{G}\left(\mathbf{x}^{(j)}, \mathbf{y}\right)$.

Proof Denote $\hat{\mathbf{y}}_1^* = \arg\min_{\mathbf{y}\in\mathbf{C}_j}\left(\hat{G}\left(\mathbf{x}^{(j)}, \mathbf{y}\right)\right)$ and $\mathbf{y}_1^* = \arg\min_{\mathbf{y}\in\mathbf{C}_j}\left(G\left(\mathbf{x}^{(j)}, \mathbf{y}\right)\right)$, i.e., $\hat{G}\left(\mathbf{x}^{(j)}, \hat{\mathbf{y}}_1^*\right)$ and $G\left(\mathbf{x}^{(j)}, \mathbf{y}_1^*\right)$ are the minimum of $\hat{G}(\mathbf{x}, \mathbf{y})$ and that of $G(\mathbf{x}, \mathbf{y})$, respectively. Note that $\hat{\mathbf{y}}_1^*$ is not necessarily equal to $\mathbf{y}_1^*$, because $\hat{G}(\mathbf{x}, \mathbf{y})$ only can exactly predict the sign of $G(\mathbf{x}, \mathbf{y})$ rather than its true value. Therefore, it is hard to directly say that $G\left(\mathbf{x}^{(j)}, \mathbf{y}_1^*\right)$ has the same sign as $\hat{G}\left(\mathbf{x}^{(j)}, \hat{\mathbf{y}}_1^*\right)$.

If $\hat{G}\left(\mathbf{x}^{(j)}, \hat{\mathbf{y}}_1^*\right) > 0$, then $\hat{G}\left(\mathbf{x}^{(j)}, \mathbf{y}_1^*\right) > 0$ because $\hat{G}\left(\mathbf{x}^{(j)}, \mathbf{y}_1^*\right) \geq \hat{G}\left(\mathbf{x}^{(j)}, \hat{\mathbf{y}}_1^*\right) > 0$. And then $G\left(\mathbf{x}^{(j)}, \mathbf{y}_1^*\right) > 0$ because $\hat{G}(\mathbf{x}, \mathbf{y})$ can rightly predict the sign of $G(\mathbf{x}, \mathbf{y})$ at the point $\left(\mathbf{x}^{(j)}, \mathbf{y}_1^*\right)$. If $\hat{G}\left(\mathbf{x}^{(j)}, \hat{\mathbf{y}}_1^*\right) < 0$, then $G\left(\mathbf{x}^{(j)}, \hat{\mathbf{y}}_1^*\right) < 0$ because $\hat{G}(\mathbf{x}, \mathbf{y})$ can rightly predict the sign of $G(\mathbf{x}, \mathbf{y})$ at the point $\left(\mathbf{x}^{(j)}, \hat{\mathbf{y}}_1^*\right)$. Then, $G\left(\mathbf{x}^{(j)}, \mathbf{y}_1^*\right) < 0$ because $G\left(\mathbf{x}^{(j)}, \mathbf{y}_1^*\right) \leq G\left(\mathbf{x}^{(j)}, \hat{\mathbf{y}}_1^*\right) < 0$. Thus, Property 1 is proved.

Property 2 *If a Kriging model* $\hat{G}(\mathbf{x}, \mathbf{y})$ *can rightly predict the sign of* $G(\mathbf{x}, \mathbf{y})$*, then the sign of* $\max_{\mathbf{y}\in\mathbf{C}_j} \hat{G}\left(\mathbf{x}^{(j)}, \mathbf{y}\right)$ *is the same as that of* $\max_{\mathbf{y}\in\mathbf{C}_j} G\left(\mathbf{x}^{(j)}, \mathbf{y}\right)$.

Proof Denote $\hat{\mathbf{y}}_2^* = \arg\max_{\mathbf{y}\in\mathbf{C}_j} \hat{G}\left(\mathbf{x}^{(j)}, \mathbf{y}\right)$ and $\mathbf{y}_2^* = \arg\max_{\mathbf{y}\in\mathbf{C}_j} G\left(\mathbf{x}^{(j)}, \mathbf{y}\right)$, namely $\hat{G}\left(\mathbf{x}^{(j)}, \hat{\mathbf{y}}_2^*\right)$ and $G\left(\mathbf{x}^{(j)}, \mathbf{y}_2^*\right)$ are the maximum of $\hat{G}(\mathbf{x}, \mathbf{y})$ and that of $G(\mathbf{x}, \mathbf{y})$, respectively. And also note that $\hat{\mathbf{y}}_2^*$ is not equal to $\mathbf{y}_2^*$ for sure. If $\hat{G}\left(\mathbf{x}^{(j)}, \hat{\mathbf{y}}_2^*\right) > 0$, then $G\left(\mathbf{x}^{(j)}, \hat{\mathbf{y}}_2^*\right) > 0$ because $\hat{G}(\mathbf{x}, \mathbf{y})$ can rightly predict the sign of $G(\mathbf{x}, \mathbf{y})$ at the point $\left(\mathbf{x}^{(j)}, \hat{\mathbf{y}}_2^*\right)$. And then $G\left(\mathbf{x}^{(j)}, \mathbf{y}_2^*\right) > 0$ because $G\left(\mathbf{x}^{(j)}, \mathbf{y}_2^*\right) \geq G\left(\mathbf{x}^{(j)}, \hat{\mathbf{y}}_2^*\right) > 0$. If $\hat{G}\left(\mathbf{x}^{(j)}, \hat{\mathbf{y}}_2^*\right) < 0$, then $\hat{G}\left(\mathbf{x}^{(j)}, \mathbf{y}_2^*\right) \leq \hat{G}\left(\mathbf{x}^{(j)}, \hat{\mathbf{y}}_2^*\right) < 0$. And then $G\left(\mathbf{x}^{(j)}, \mathbf{y}_2^*\right) < 0$ because $\hat{G}(\mathbf{x}, \mathbf{y})$ can

rightly predict the sign of $G(\mathbf{x}, \mathbf{y})$ at the point $\left(\mathbf{x}^{(j)}, \mathbf{y}_2^*\right)$. That is the sign of $\max_{\mathbf{y}\in\mathbf{C}_j} \hat{G}\left(\mathbf{x}^{(j)}, \mathbf{y}\right)$ is the same as that of $\max_{\mathbf{y}\in\mathbf{C}_j} G\left(\mathbf{x}^{(j)}, \mathbf{y}\right)$. Property 2 is proved.

From Properties 1 and 2, it is known that extrema of $G(\mathbf{x}, \mathbf{y})$ have the same signs with those of $\hat{G}(\mathbf{x}, \mathbf{y})$ at each simulated sample as long as $\hat{G}(\mathbf{x}, \mathbf{y})$ can rightly predict the sign of $G(\mathbf{x}, \mathbf{y})$. Obtaining the signs of extrema of $\hat{G}(\mathbf{x}, \mathbf{y})$, the signs of extrema of $G(\mathbf{x}, \mathbf{y})$ will be obtained at each simulated sample. Therefore, rightly predicting the sign of performance function can satisfy the demand of accuracy for HRA.

It should be noted that several works have realized that rightly predicting the sign of performance function can satisfy the demand of accuracy in probability reliability analysis (PRA) [39–41]. However, people cannot take it for granted that this claim holds true in HRA. That is because only rightly predicting the sign cannot assure rightly predicting the optimal solutions of extrema and cannot assure rightly predicting the sign of extrema. Through Properties 1 and 2, we have proved this claim holds true for HRA.

Then, we will focus on how to construct an ALK model to rightly predicting the sign of performance function in HRA. It should be noted that several strategies have been proposed to improve the prediction for the sign of performance function based on Kriging model [39–44]. However, to our best knowledge, all of them are proposed for PRA. In this paper, we propose an ALK model to predict the sign of performance function with both random and p-box variables. ALK-OIMCS is proposed for HRA while others were proposed for PRA. Therefore, the detailed comparison with other strategies is beyond our scope.

The general procedure to build an ALK model is outlined as follows [39,45,46]:

(1) Construct an initial Kriging model with a small number of training points.
(2) Identify the point which maximizes a learning function. The learning function is a function to find a point that probably locates in some region of interest. If the value of learning function at this point satisfies some prescribed tolerance, stop.
(3) Evaluate the objective function at this point and add it into the set of training points. Build a new Kriging model and return to Step (2).

During that procedure, a learning function plays the leading role for an ALK model. It determines which point should be added into the set of training points and when the iterative process should be stopped. In the study [47], elaborated a brand new learning function called expected risk function (ERF) [47]. Based on ERF, ALK-OIMCS is constructed.

4.2 Remainder of Kriging model

For simplicity, we use the vector $\mathbf{u}$ to replace $(\mathbf{x}, \mathbf{y})$, then the performance function becomes $G(\mathbf{u})$. Kriging models $G(\mathbf{u})$ by

$$G(\mathbf{u}) = F(\mathbf{u}, \boldsymbol{\beta}) + z(\mathbf{u}), \tag{13}$$

where $F(\mathbf{u}, \boldsymbol{\beta})$ is the polynomial regression part and $\boldsymbol{\beta}$ is the vector of regression coefficients. In this paper, ordinary Kriging modelling [48] is adopted which means that $F(\mathbf{u}, \boldsymbol{\beta})$ is a constant and $F(\mathbf{u}, \boldsymbol{\beta}) = \beta^*$. $z(\mathbf{u})$ is a Gaussian random process whose mean and covariance are defined as

$$\begin{cases} E\left[z(\mathbf{u})\right] = 0 \\ \operatorname{cov}\left[z(\mathbf{a}), z(\mathbf{b})\right] = \sigma^2 \Re(\boldsymbol{\theta}, \mathbf{a}, \mathbf{b}) \end{cases} \tag{14}$$

in which $\mathbf{a}$ and $\mathbf{b}$ are two arbitrary points, σ^2 is the process variance, $\Re(\cdot)$ is a correlation function with parameter $\boldsymbol{\theta}$.

Several models are available to define the correlation function. The Gaussian correlation function is selected, which is defined as

$$\Re(\boldsymbol{\theta}, \mathbf{a}, \mathbf{b}) = \exp\left[-\sum_{i=1}^{n} \theta_i (a_i - b_i)^2\right], \tag{15}$$

where a_i, b_i and θ_i are the ith coordinates of $\mathbf{a}$, $\mathbf{b}$ and $\boldsymbol{\theta}$, respectively.

The Kriging model entails a DoE to define its stochastic parameters. Then predictions can be done at unknown points. Given a DoE: $\left[\mathbf{u}^{(1)}, \mathbf{u}^{(2)}, \ldots, \mathbf{u}^{(m)}\right]^T$ with $\mathbf{u}^{(i)}$ the ith training point, and $\mathbf{G} =$

$\left[G(\mathbf{u}^{(1)}), G(\mathbf{u}^{(2)}), \ldots, G(\mathbf{u}^{(m)})\right]^T$ with $G\left(\mathbf{u}^{(i)}\right)$ the ith function value, the predicted value $\hat{G}(\mathbf{u})$ and predicted variance $s^2(\mathbf{u})$ for $G(\mathbf{u})$ are, respectively, given by

$$\hat{G}(\mathbf{u}) = \beta^* + \mathbf{r}(\mathbf{u})^T \mathbf{R}^{-1}\left(\mathbf{G} - \mathbf{1}\beta^*\right) \tag{16}$$

and

$$s^2(\mathbf{u}) = \sigma^2\left[1 - \mathbf{r}^T(\mathbf{u})\mathbf{R}^{-1}\mathbf{r}(\mathbf{u}) + \frac{\left(1 - \mathbf{1}^T\mathbf{R}^{-1}\mathbf{r}(\mathbf{u})\right)^2}{\mathbf{1}^T\mathbf{R}^{-1}\mathbf{1}}\right]. \tag{17}$$

In Eq. (16),

$$\beta^* = \left(\mathbf{1}^T\mathbf{R}^{-1}\mathbf{1}\right)^{-1}\mathbf{1}^T\mathbf{R}^{-1}\mathbf{G}, \tag{18}$$

$$\mathbf{r}(\mathbf{u}) = \left[\Re(\boldsymbol{\theta}, \mathbf{u}, \mathbf{u}^{(1)}), \Re(\boldsymbol{\theta}, \mathbf{u}, \mathbf{u}^{(2)}), \ldots, \Re(\boldsymbol{\theta}, \mathbf{u}, \mathbf{u}^{(m)})\right]^T. \tag{19}$$

In Eqs. (16–17), $\mathbf{R}$ is an $m \times m$ matrix with

$$R_{ij} = \Re\left(\boldsymbol{\theta}, \mathbf{u}^{(i)}, \mathbf{u}^{(j)}\right). \tag{20}$$

In Eq. (17),

$$\sigma^2 = \frac{1}{m}\left(\mathbf{G} - \beta^*\mathbf{1}\right)^T\mathbf{R}^{-1}\left(\mathbf{G} - \mathbf{1}\beta^*\right). \tag{21}$$

The parameter $\boldsymbol{\theta}$ in Eq. (20) should be determined through maximum likelihood estimation. Thus, the unconstrained optimization problem needs to be worked out as follows:

$$\boldsymbol{\theta}^* = \arg\min_{\boldsymbol{\theta}}\left(|\mathbf{R}|^{\frac{1}{m}}\sigma^2\right). \tag{22}$$

The ALK models in Refs. [40,49] are all performed in the MATLAB toolbox DACE [50]. In DACE, a pattern search method is utilized to find $\boldsymbol{\theta}^*$ in Eq. (22). However, this method is prone to become trapped in local minima [51]. As explained in Ref. [52], θ has the greatest influence on the Kriging model. Only the Kriging model with the globally optimal parameter $\boldsymbol{\theta}^*$ can provide the best predictions in Eqs. (16) and (17). Therefore, the optimization in Eq. (22) is solved by global optimization strategy, and the algorithm adopted is the DIRECT algorithm [38] in this paper.

4.3 EIF for EGO

ERF [47] is proposed inspired by the so-called expected improvement function (EIF) which was elaborated to find the global minimum in global optimization [46,47]. Therefore, EIF is simply introduced in this subsection. EIF was proposed based on the idea that how to recognize the point whose function value has the largest improvement than the current optimum. To do so, an indicator to measure the improvement at an arbitrary point $\mathbf{u}$ was defined by

$$I(\mathbf{u}) = \max\left(G_{\min} - G(\mathbf{u}), 0\right), \tag{23}$$

where $G_{\min}$ is the minimum response among the current DoE. Realizing that $G(\mathbf{u}) \sim N\left(\hat{G}(\mathbf{u}), s(\mathbf{u})\right)$ [45,46], the indicator $I(\mathbf{u})$ is averaged in the real domain and the expectation of $I(\mathbf{u})$ is obtained as

$$\begin{aligned} E\left[I(\mathbf{u})\right] &= E\left[\max\left(G_{\min} - G(\mathbf{u}), 0\right)\right] \\ &= \int_{-\infty}^{G_{\min}}\left(G_{\min} - G(\mathbf{u})\right)\phi\left(\frac{G(\mathbf{u}) - \hat{G}(\mathbf{u})}{s(\mathbf{u})}\right)\mathrm{d}G \\ &= \left(G_{\min} - \hat{G}(\mathbf{u})\right)\Phi\left(\frac{G_{\min} - \hat{G}(\mathbf{u})}{s(\mathbf{u})}\right) + s(\mathbf{u})\phi\left(\frac{G_{\min} - \hat{G}(\mathbf{u})}{s(\mathbf{u})}\right), \end{aligned} \tag{24}$$

where $\Phi(\cdot)$ is the standard normal CDF and $\phi(\cdot)$ is the standard normal PDF. Equation (24) is named as EIF in [46].

4.4 ALK-OIMCS

4.4.1 Expected risk function

EIF [46] was proposed for searching the minimum of the objective function in global optimization. But in HRA, we have a different purpose. Our goal is to construct a Kriging model rightly predicting the sign of $G(\mathbf{u})$. To fulfill this task, it is required to indentify the point at which the sign of objective function has the largest risk of being wrongly predicted. Add this point to the DoE, and then the prediction for the sign of $G(\mathbf{u})$ will be improved. Based on this natural idea, we elaborated ERF in the study [47].

At an unknown point $\mathbf{u}$, the Kriging model provides a predicted value $\hat{G}(\mathbf{u})$ for $G(\mathbf{u})$. However, $\hat{G}(\mathbf{u})$ is not the exact value, and there exists some uncertainty for this prediction. Hereby, some risk occurs that the prediction for the sign of $G(\mathbf{u})$ is wrong.

Consider the case that the Kriging model gives a negative sign, i.e., $\hat{G}(\mathbf{u}) < 0$. Although $\hat{G}(\mathbf{u}) < 0$, there still exists some risk that $G(\mathbf{u})$ is positive, i.e., $G(\mathbf{u}) > 0$, because $G(\mathbf{u})$ is uncertain and $G(\mathbf{u}) \sim N\left(\hat{G}(\mathbf{u}), s(\mathbf{u})\right)$. We define an indicator to measure such risk as

$$R(\mathbf{u}) = \max\left[\left(G(\mathbf{u}) - 0\right), 0\right]. \tag{25}$$

$R(\mathbf{u})$ indicates how much $G(\mathbf{u})$ is larger than zero if $\hat{G}(\mathbf{u}) < 0$ or how severely the true sign of $G(\mathbf{u})$ violates that of the prediction. Obviously, as depicted in Fig. 3a, the larger $R(\mathbf{u})$ is, the easier the sign of $G(\mathbf{u})$ is to be wrongly predicted. Similarly as EIF, we average $R(\mathbf{u})$ over the real space, and the expectation of $R(\mathbf{u})$ in the case $\hat{G}(\mathbf{u}) < 0$ is derived as

$$E\left[R(\mathbf{u})\right] = s(\mathbf{u})\phi\left(\frac{\hat{G}(\mathbf{u})}{s(\mathbf{u})}\right) + \hat{G}(\mathbf{u})\Phi\left(\frac{\hat{G}(\mathbf{u})}{s(\mathbf{u})}\right). \tag{26}$$

Similarly, as shown in Fig. 3b, we define the risk for the case $\hat{G}(\mathbf{u}) > 0$ as

$$R(\mathbf{u}) = \max\left[\left(0 - G(\mathbf{u})\right), 0\right]. \tag{27}$$

And the expectation of $R(\mathbf{u})$ in the case $\hat{G}(\mathbf{u}) > 0$ is derived as

$$E\left[R(\mathbf{u})\right] = -\hat{G}(\mathbf{u})\Phi\left(-\frac{\hat{G}(\mathbf{u})}{s(\mathbf{u})}\right) + s(\mathbf{u})\phi\left(\frac{\hat{G}(\mathbf{u})}{s(\mathbf{u})}\right). \tag{28}$$

Eqs. (26) and (28) can be written into a uniform equation as

$$E\left[R(\mathbf{u})\right] = -\text{sign}\left(\hat{G}(\mathbf{u})\right)\hat{G}(\mathbf{u})\Phi\left(-\text{sign}\left(\hat{G}(\mathbf{u})\right)\frac{\hat{G}(\mathbf{u})}{s(\mathbf{u})}\right) + s(\mathbf{u})\phi\left(\frac{\hat{G}(\mathbf{u})}{s(\mathbf{u})}\right), \tag{29}$$

where sign$(\cdot)$ is the sign function.

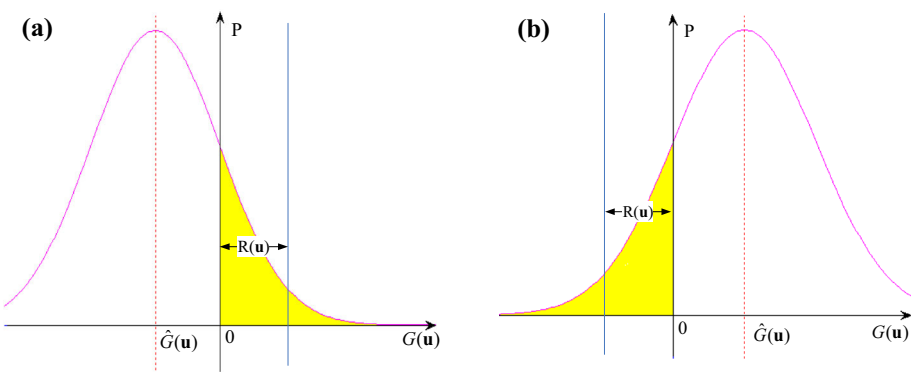

Fig. 3 Risk of the sign wrongly predicted by a Kriging model: **(a)** case of negative prediction; **(b)** case of positive prediction

Equation (29) is named ERF in this paper. ERF measures the extent of risk that a Kriging model wrongly predicts the sign of objective function at a point. The point with maximum ERF indicates the sign of objective function at this point has the largest risk to be wrongly predicted. So, it should be added to the DoE in ALK-OIMCS.

4.4.2 Procedure of ALK-OIMCS

(1) Generate a large amount of samples as candidate points.
   (a) The performance function is evaluated at none of the points at this stage. These points are all treated as candidate points, and the added training points will be picked out among them.
   (b) The set of candidate points is denoted as Θ. For random variables, samples are generated by virtue of LSM according to the probabilistic distributions of the random variables. For p-box variables, the approximating space should envelop all the interval samples obtained in Sect. 3. Latin hypercube sampling (LHS) is employed to generate samples uniformly spanning the space, and the lower and upper bounds are chosen as $\underline{\mathbf{C}} = \min_{j=1}^{N} \underline{\mathbf{y}}^{(j)}$ and $\overline{\mathbf{C}} = \max_{j=1}^{N} \overline{\mathbf{y}}^{(j)}$, respectively.
   (c) The number of candidate points should be large enough to fill every part of the uncertain space. We choose 10^5 in this paper.
(2) Define the initial DoE and build the initial Kriging model.
   (a) The number of the initial training points is preferred to be defined small. Considering the experience stated in Ref. [40], we make the number as 12 in this paper.
   (b) LHS is used to generate the samples and thus they can uniformly distribute in the uncertain space. For random variables, the bounds are chosen as $F_{\mathbf{X}}^{-1}[\Phi(\pm 5)]$. For p-box variables, the bounds are chosen the same as in Stage (1).
   (c) Compute the performance function at all of the points and build a Kriging model with the initial DoE.
(3) Identify the next point to be added into the DoE.
   The point among Θ which maximizes ERF is chosen as the next point and denote it as $\left(\mathbf{x}^{(*)}, \mathbf{y}^{(*)}\right)$.
(4) Stopping condition.
   If the maximum ERF is small enough, the Kriging model has been accurate enough to approximate the sign of performance function. Go to Stage (6). Inspecting Eq. (29), it can be seen that ERF is a dimensional function depending on the value of performance function. This could impact the convergence of iteration for different performance functions. To decrease this influence, ERF is scaled by the maximum absolute value of performance function in the initial DoE. Thus, the stopping condition is $E\left[R\left(\mathbf{x}^{(*)}, \mathbf{y}^{(*)}\right)\right] / \max_{i=1}^{12} \left|G\left(\mathbf{x}^{(i)}, \mathbf{y}^{(i)}\right)\right| \leq 10^{-5}$.
(5) Update the DoE and the Kriging model.
   If the stopping condition is not satisfied in Stage (4), evaluate the performance function at $\left(\mathbf{x}^{(*)}, \mathbf{y}^{(*)}\right)$. Add this point into the DoE and build a new Kriging model. Go to Stage (3).
(6) This surrogate model is accurate enough to predict the sign of performance function. Carry out OIMCS based on the Kriging model and obtain both the lower and upper bounds of failure probability.

5 Numerical examples and discussion

5.1 A mathematical problem

A numerical problem from Ref. [39] is considered. The performance function is defined as

$$G(\mathbf{x}, \mathbf{y}) = 2 - \frac{(x-1)\left(y^2+4\right)}{20} + \sin\left(\frac{5y}{2}\right), \tag{30}$$

where x is a normal variable and y is a p-box variable. Details about them are listed in Table 1. The performance function is highly nonlinear and multimodal with respect to the p-box variable.

Table 1 Uncertain variables of the mathematical problem

Variables	Distribution type	Mean	Standard deviation
x	Normal	2.5	1
y	Normal	[1.4, 1.6]	[0.9, 1.1]

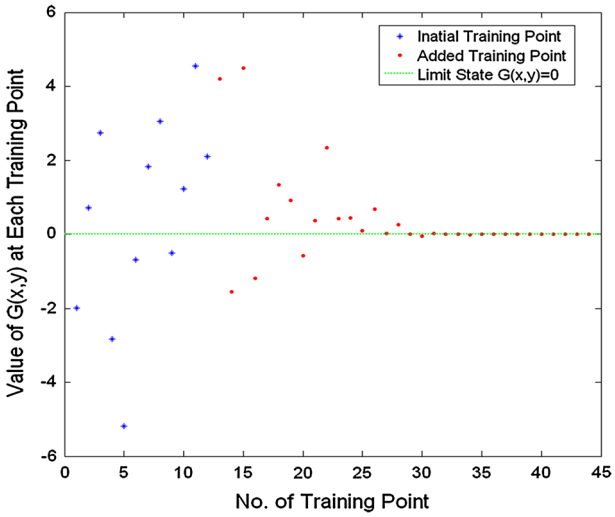

Fig. 4 DoE obtained with ALK-OIMCS for the mathematical problem

Table 2 Results of the mathematical problem using different methods

Method	$\overline{P}_f$	$\underline{P}_f$	Function calls	Error (upper bound/lower bound)
OIMCS	0.05330	0.01399	$2 \times 100 \times 10^5$	–
ALK-OIMCS	0.05329	0.01400	44	0.020/0.07 %

ALK-OIMCS is utilized to calculate the bounds of failure probability for this problem. Firstly, a Kriging model should be built to exactly predict the sign of $G(\mathbf{x}, \mathbf{y})$. A total of 12 training points are utilized to construct an initial Kriging model and then the iterative process starts. After 32 iterations, the stopping condition is satisfied. A total of 32 training points are added into the initial DoE, and the Kriging model is updated for 32 times. The DoE obtained is shown in Fig. 4. It can be seen that a large amount of the added points concentrates on the vicinity of $G(\mathbf{x}, \mathbf{y}) = 0$. That indicates that ALK-OIMCS only locally approximates the performance function in the interesting region rather than in the whole space. To approximate this highly nonlinear performance function, only 44 function calls are needed. That shows the efficiency of the proposed method.

After the Kriging model is created, OIMCS can be implemented based on the Kriging model. $\mathrm{N} = 10^5$ simulated samples are sampled with LSM, and the extrema of $G(\mathbf{x}, \mathbf{y})$ are repeatedly searched at every sample. The results are shown in Table 2. To verify the results of proposed method, OIMCS based on the true performance function are also carried out with the same simulated samples. It can be seen from Table 2 that for this highly nonlinear problem, ALK-OIMCS provides pretty accurate results with less than 1 % errors.

5.2 A 10-bar truss

A 10-bar truss [53] shown in Fig. 5 is considered in this section. The Young's Modulus is 10^5 MPa. The truss structure is subjected to a vertical load F_1 at node 4, a vertical load F_2 and a horizontal load F_3 at node 2. The cross-sectional area of the bars 1–4, that of the bars 5–6, and that of the rest ones equal to A_1, A_2, A_3, respectively. The vertical deflection at node 2 should be less than 9.5 mm, so the performance function is constructed as

$$G(\mathbf{x}, \mathbf{y}) = 9.5 - \Delta_2, \tag{31}$$

where Δ_2 is the vertical defection of node 2, which is obtained by FE codes programmed in Matlab. In this problem, A_1, A_2, A_3 and F_1, F_2, F_3 are treated as uncertain variables. Details are shown in Table 3.

Results of this problem obtained by OIMCS and ALK-OIMCS are listed in Table 4. It is seen that the proposed method performs very well no matter in efficiency or accuracy. It obtains very accurate bounds of failure probability with only 50 function calls. The DoE obtained by ALK-OIMCS is illustrated in Fig. 6. It can be seen that a large portion of training points falls in the vicinity of $G(\mathbf{x}, \mathbf{y}) = 0$. Therefore, ALK-OIMCS only

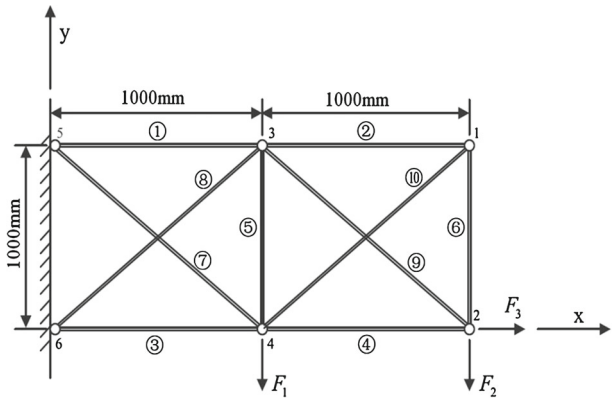

Fig. 5 A 10-bar truss

Table 3 Uncertain variables of the 10-bar truss

Variables	Distribution type	Mean	Standard deviation
A_1/mm^2	Normal	1,000	50
A_2/mm^2	Normal	1,000	50
A_3/mm^2	Normal	1,000	50
F_1/kN	Normal	[79.5, 80.5]	[1.9, 2.1]
F_2/kN	Normal	[79.5, 80.5]	[1.9, 2.1]
F_3/kN	Normal	[9.9, 10.1]	[0.49, 0.51]

Table 4 Results of the10-bar truss using different methods

Method	$\overline{P}_f$	$\underline{P}_f$	Function calls	Error (upper bound/lower bound)
OIMCS	0.01124	0.00388	$2 \times 400 \times 10^5$	–
ALK-OIMCS	0.01119	0.00387	50	0.44/0.26 %

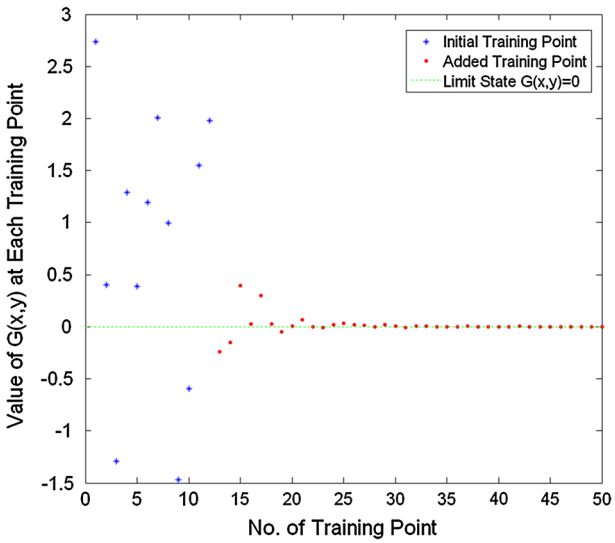

Fig. 6 DoE obtained with ALK-OIMCS for the10-bar truss

locally approximates $G(\mathbf{x}, \mathbf{y})$ rather than throughout the uncertain space. Moreover, when the single Kriging model is constructed, it can be used to estimate both bounds of failure probability. That is why ALK-OIMCS can be so efficient.

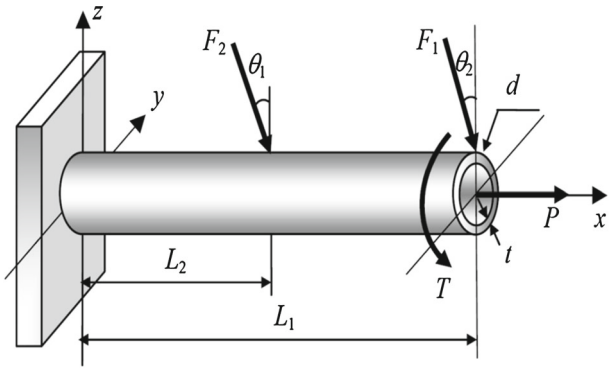

Fig. 7 A cantilever tube [30]

Table 5 Uncertain variables of the cantilever tube

Variables	Distribution type	Parameter1	Parameter2
t/mm	Normal	5	0.1
d/mm	Normal	42	0.5
L_2/mm	Uniform	59.75	60.25
F_1/N	Gumbel	3,000	300
F_2/N	Gumbel	3,000	300
P/N	Normal	12,000	1,200
T/N m	Normal	90	9
L_1/mm	Normal	[119, 121]	[0.04, 0.06]
θ_1/°	Normal	[4.9, 5.1]	[0.85, 0.95]
θ_2/°	Normal	[9.9, 10.1]	[0.95, 1.05]

For normal distribution, parameter 1 and 2 are the mean and standard deviation, respectively; for uniform distribution, parameter 1 and 2 refer to the lower and upper bounds, respectively; for the Gumbel distribution, parameter 1 and 2 are the location parameter and scale parameter, respectively

5.3 A cantilever tube

The third example is a cantilever tube from Ref. [30]. As shown in Fig. 7, three external forces F_1, F_2, P and a torsion T are exerted on the tube. The maximum Von Mises stress $\sigma_{\max}$ in the tube should be less than 180 MPa, so the performance function is created as

$$G(\mathbf{x}, \mathbf{y}) = 180 - \sigma_{\max}, \tag{32}$$

where $\sigma_{\max}$ can be computed by

$$\sigma_{\max} = \sqrt{\sigma_x^2 + 3\tau_{zx}^2}. \tag{33}$$

The normal stress σ_x and torsional stress τ_{zx} are, respectively, calculated by

$$\sigma_x = \frac{P + F_1 \sin(\theta_1) + F_2 \sin(\theta_2)}{A} + \frac{Md}{2I}, \tag{34}$$

$$\tau_{zx} = \frac{Td}{4I}, \tag{35}$$

and we have

$$\begin{cases} M = F_1 L_1 \cos(\theta_1) + F_2 L_2 \cos(\theta_2), \\ A = \frac{\pi}{4}[d^2 - (d-2t)^2], \\ I = \frac{\pi}{64}[d^4 - (d-2t)^4]. \end{cases} \tag{36}$$

Random and p-box variables of the cantilever tube are given in Table 5. Note that the performance function is not monotonic in terms of θ_1 and θ_2 as shown in Ref. [30].

The bounds of failure probability for this problem are estimated in ALK-OIMCS. The DoE obtained is illustrated in Fig. 8. It is shown that the main part of training points focus on the neighborhood of $G(\mathbf{x}, \mathbf{y}) = 0$. ALK-OIMCS obtains the results with calling the performance function only 59 times. To verify the results,

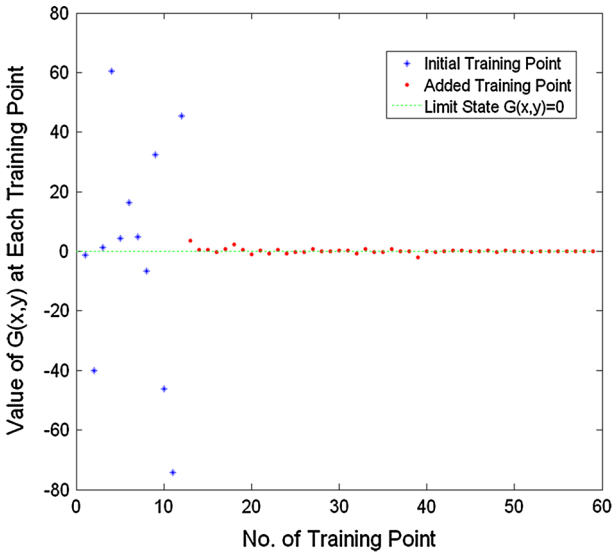

Fig. 8 DoE obtained with ALK-OIMCS for the cantilever tube

Table 6 Results of the cantilever tube using different methods

Method	$\overline{P}_f$	$\underline{P}_f$	Function calls	Error (upper bound/lower bound)
OIMCS	0.00550	0.00417	$2 \times 400 \times 10^5$	–
ALK-OIMCS	0.00553	0.00412	59	0.55/1.2 %

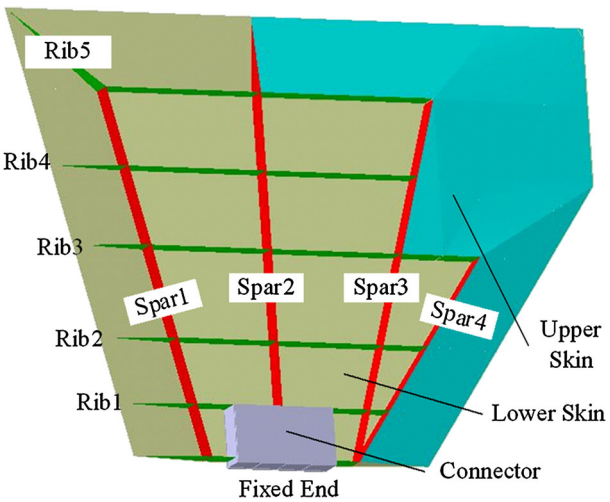

Fig. 9 A missile wing structure

OIMCS is implemented based on the true performance function. $N = 10^5$ samples are used, and 800 function calls are needed to obtain the lower and upper bounds of the performance function by the DIRECT algorithm at each simulated sample. In total, 8×10^7 function evaluations are entailed with OIMCS. Results of this problem with those two methods are listed in Table 6. For this complicated problem, ALK-OIMCS obtains the results with very little errors. That shows the high efficiency and accuracy of the proposed method.

5.4 A missile wing structure

A missile wing structure is studied in this section. As shown in Fig. 9, the missile wing structure is mainly made up of the upper and lower skins, five wing ribs and four wing spars. It is fixed on a connector which is on the missile body. Note that in Fig. 9 the upper skin is partially hidden to illustrate the inner details of the wing.

Table 7 Uncertain variables of the missile wing structure

Variables	Distribution type	Mean	Standard deviation
t_1/mm	Normal	2	0.1
t_2/mm	Normal	2	0.1
t_3/mm	Normal	2	0.1
t_4/mm	Normal	2	0.1
t_5/mm	Normal	2	0.1
t_6/mm	Normal	2	0.1
t_7/mm	Normal	2	0.1
t_8/mm	Normal	2	0.1
t_9/mm	Normal	2	0.1
s_1/mm	Normal	1	0.05
s_2/mm	Normal	1	0.05
E_1/GPa	Normal	[69.75, 70.25]	[0.14, 0.16]
E_2/GPa	Normal	[117.5, 117.7]	[0.14, 0.16]
P/MPa	Normal	[0.149, 0.151]	[0.0005, 0.0007]

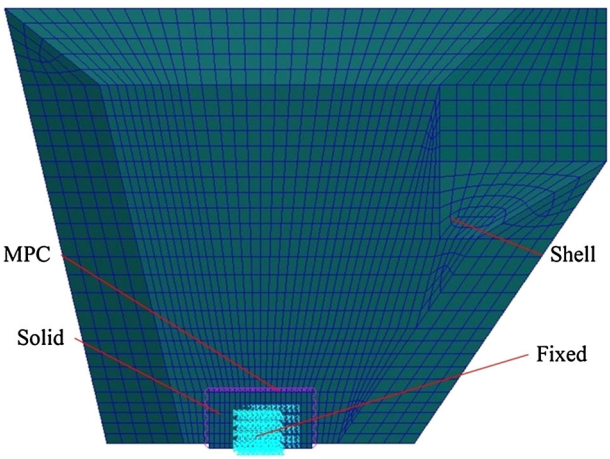

Fig. 10 FE model of the missile wing structure

The skins are all made of some kind of material with the Young's modulus E_1, the density 2.0×10^3 kg/m^3 and the Poisson's ratio 0.3. The spars and ribs are all made of titanium alloy with the Young's modulus E_2, the density 4.5×10^3 kg/m^3 and the Poisson's ratio 0.3. A uniform air pressure P is applied on the upper skin during flight. The thicknesses of wing spars and ribs are denoted as t_i $(i = 1, \ldots, 9)$. The thicknesses of the skins are represented by s_1 and s_2.

In this problem, E_1, E_2, s_1, s_2, P and t_i $(i = 1, \ldots, 9)$ are assumed to be uncertain variables. Details of them are given in Table 7. To guarantee the accuracy of missile flight path, the deformation of the wing should not exceed an allowable value. Thus, the performance function is created as

$$G(\mathbf{x}, \mathbf{y}) = d_m - d(\mathbf{x}, \mathbf{y}), \tag{37}$$

where d_m is the allowable value of the vertical deformation which is set to be 8.8 mm, d is the vertical deformation of the wing which entails to be calculated by FE analysis, the vector $\mathbf{x}$ and $\mathbf{y}$, respectively, denote all the random variables and all the p-box variables.

The FE model, as shown in Fig. 10, is created in MSC.Patran software. The spars, ribs and skins are meshed into 4,063 shell elements, and the connector is meshed into 840 solid elements. The connection between the shell elements and solid elements is simulated with 80 MPC elements. Partial solid elements are constrained by six freedom degrees and a uniform pressure is applied on the upper skin. The vertical deformation of the missile wing structure is calculated with MSC.Nastran software.

The engineering problem is solved with the proposed method. The interval of failure probability obtained is [0.00255, 0.05656]. For this complex engineering problem, ALK-OIMCS obtains this result with calling MSC.Nastran only 116 times. The DoE obtained with ALK-OIMCS is shown in Fig. 11. Again it is observed that the proposed method only finely approximates the performance function in the region of interest. In

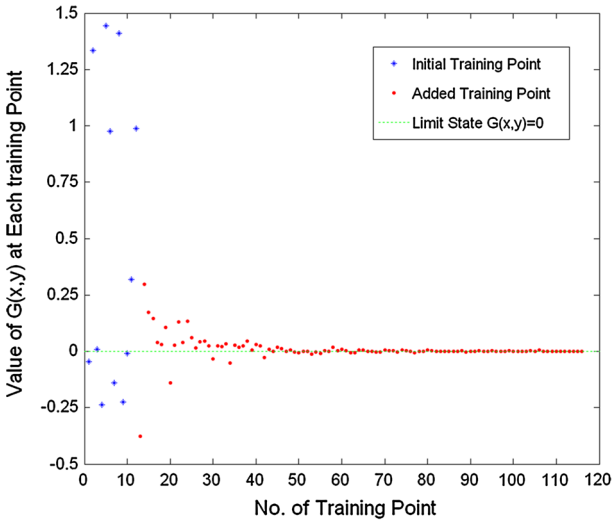

Fig. 11 DoE obtained with ALK-OIMCS of the missile wing structure

addition, both the lower and upper bounds of failure probability can be estimated by the single Kriging model. That is why the proposed method can be so efficient. From this case study, it is demonstrated that ALK-OIMCS is applicable to coping with many complicated engineering problems with implicit performance functions.

6 Conclusion

In this paper, we propose a method based on active learning Kriging model to deal with HRA with both random and *p*-box variables. First of all, it is figured out that a Kriging model able to exactly predict the sign of performance function can satisfy the demand of accuracy. Then, the method named ALK-OIMCS is proposed based on that idea. When constructing the Kriging model, the proposed method only approximates the performance function with random and *p*-box variables in the region where the sign tends to be wrongly predicted. Then, OIMCS can be effectively performed to calculate both the lower and upper bounds of failure probability based on this Kriging model.

Three numerical examples are examined with the proposed method. It is demonstrated that the proposed method behaves very well no matter in efficiency or accuracy. ALK-OIMCS could obtain very precise results with calling the performance function as few times as possible. The high accuracy of ALK-OIMCS in return validates our main claim that a Kriging model just able to exactly predict the sign of performance function can meet the demand of accuracy for HRA. From the last engineering problem, it is shown that ALK-OIMCS is a very efficient technique that is competent to deal with many complex engineering problems with implicit performance functions.

Acknowledgments This work is supported by the Aerospace Support Fund (NBXW0001), the Foundation Research Funds of Northwestern Polytechnical University (JC201114) and Aviation Science Foundation (2011ZA53014).

References

1. Helton, J.C.: Uncertainty and sensitivity analysis in the presence of stochastic and subjective uncertainty. J. Stat. Comput. Simul. **57**, 3–76 (1997)
2. Bae, H.R., Grandhi, R.V., Canfield, R.A.: Epistemic uncertainty quantification techniques including evidence theory for large-scale structures. Comput. Struct. **82**, 1101–1112 (2004)
3. Der Kiureghian, A.: Analysis of structural reliability under parameter uncertainties. Probab. Eng. Mech. **23**, 351–358 (2008)
4. Choi, J., An, D., Won, J.: Bayesian approach for structural reliability analysis and optimization using the Kriging Dimension Reduction Method. J. Mech. Des. **132**, 051003 (2010)
5. Davis, J.P., Hall, J.W.: A software-supported process for assembling evidence and handling uncertainty in decision-making. Decis. Support Syst. **35**, 415–433 (2003)
6. Augustin, T.: Optimal decisions under complex uncertainty-basic notions and a general algorithm for data-based decision making with partial prior knowledge described by interval probability. ZAMM-J. Appl. Math. Mech. **84**, 678–687 (2004)

7. Troffaes, M.C.M., Miranda, E., Destercke, S.: On the connection between probability boxes and possibility measures. Inf. Sci. **224**, 88–108 (2013)
8. Crespo, L.G., Kenny, S., Giesy, D.: Reliability analysis of polynomial systems subject to p-box uncertainties. Mech. Syst. Signal Process. **37**, 121–136 (2013)
9. Jiang, C., Zhang, Z., Han, X., Liu, J.: A novel evidence-theory-based reliability analysis method for structures with epistemic uncertainty. Comput. Struct. **129**, 1–12 (2013)
10. Beer, M., Ferson, S.: Fuzzy probability in engineering analyses. In: Proceedings of the First International Conference on Vulnerability and Risk Analysis and Management (ICVRAM 2011) and the Fifth International Symposium on Uncertainty Modeling and Analysis (ISUMA 2011) (2011)
11. Hurtado, J.E., Alvarez, D.A., Ramírez, J.: Fuzzy structural analysis based on fundamental reliability concepts. Comput. Struct. **112**, 183–192 (2012)
12. Jiang, C., Bi, R.G., Lu, G.Y., Han, X.: Structural reliability analysis using non-probabilistic convex model. Comput. Methods Appl. Mech. Eng. **254**, 83–98 (2013)
13. Luo, Y.J., Alex, L., Kang, Z.: Reliability-based design optimization of adhesive bonded steel–concrete composite beams with probabilistic and non-probabilistic uncertainties. Eng. Struct. **33**, 2110–2119 (2011)
14. Elishakoff, I.: Essay on uncertainties in elastic and viscoelastic structures: from AM Freudenthal's criticisms to modern convex modeling. Comput. Struct. **56**, 871–895 (1995)
15. Beer, M., Ferson, S., Kreinovich, V.: Imprecise probabilities in engineering analyses. Mech. Syst. Signal Process. **37**, 4–29 (2013)
16. Ferson, S., Kreinovich, V., Ginzburg, L., Myers, D.S., Sentz, K.: Constructing probability boxes and Dempster–Shafer structures, vol. 835. Sandia National Laboratories, Albuquerque (2002)
17. Alvarez, D.A.: On the calculation of the bounds of probability of events using infinite random sets. Int. J. Approx. Reason. **43**, 241–267 (2006)
18. Alvarez, D.A.: A Monte Carlo-based method for the estimation of lower and upper probabilities of events using infinite random sets of indexable type. Fuzzy Sets Syst. **160**, 384–401 (2009)
19. Batarseh, O.G., Wang, Y.: Reliable simulation with input uncertainties using an interval-based approach. In: Simulation Conference, 2008. WSC 2008. Winter 2008, pp. 344–352
20. Zhang, H., Mullen, R.L., Muhanna, R.L.: Interval Monte Carlo methods for structural reliability. Struct. Saf. **32**, 183–190 (2010)
21. Zhang, H.: Interval importance sampling method for finite element-based structural reliability assessment under parameter uncertainties. Struct. Saf. **38**, 1–10 (2012)
22. Zhang, H., Dai, H., Beer, M., Wang, W.: Structural reliability analysis on the basis of small samples: an interval quasi-Monte Carlo method. Mech. Syst. Signal Process. **37**, 137–151 (2013)
23. Jiang, C., Li, W.X., Han, X., Liu, L.X., Le, P.H.: Structural reliability analysis based on random distributions with interval parameters. Comput. Struct. **89**, 2292–2302 (2011)
24. Hurtado, J.E.: Assessment of reliability intervals under input distributions with uncertain parameters. Probab. Eng. Mech. **32**, 80–92 (2013)
25. Xiao, N.C., Huang, H.Z., Wang, Z., Pang, Y., He, L.: Reliability sensitivity analysis for structural systems in interval probability form. Struct. Multidisc. Optim. **44**, 691–705 (2011)
26. Qiu, Z., Yang, D., Elishakoff, I.: Probabilistic interval reliability of structural systems. Int. J. Solids Struct. **45**, 2850–2860 (2008)
27. Eldred, M.S., Swiler, L.P., Tang, G.: Mixed aleatory-epistemic uncertainty quantification with stochastic expansions and optimization-based interval estimation. Reliab. Eng. Syst. Saf. **96**, 1092–1113 (2011)
28. Du, X.: Reliability-based design optimization with dependent interval variables. Int. J. Numer. Methods Eng. **91**, 218–228 (2012)
29. Luo, Y.J., Kang, Z., Alex, L.: Structural reliability assessment based on probability and convex set mixed model. Comput. Struct. **87**, 1408–1415 (2009)
30. Du, X.: Unified uncertainty analysis by the first order reliability method. J. Mech. Des. **130**, 091401–091410 (2008)
31. Yao, W., Chen, X., Huang, Y., Tooren, M.: An enhanced unified uncertainty analysis approach based on first order reliability method with single-level optimization. Reliab. Eng. Syst. Saf. **116**, 28–37 (2013)
32. Balu, A.S., Rao, B.N.: Multicut-high dimensional model representation for structural reliability bounds estimation under mixed uncertainties. Comput. Aid. Civ. Infrastruct. Eng. **27**, 419–438 (2012)
33. Guo, J., Du, X.: Sensitivity analysis with mixture of epistemic and aleatory uncertainties. AIAA J. **45**, 2337–2349 (2007)
34. Moens, D., Hanss, M.: Non-probabilistic finite element analysis for parametric uncertainty treatment in applied mechanics: Recent advances. Finite Elem. Anal. Des. **47**, 4–16 (2011)
35. Ang, A., Tang, W.: Probability Concepts in Engineering Planning and Design, vol. 1. Wiley, New York (1975)
36. Dai, H., Wang, W.: Application of low-discrepancy sampling method in structural reliability analysis. Struct. Saf. **31**, 55–64 (2009)
37. Vanhatalo, J.: GPstuff: Gaussian process models for Bayesian analysis V2.0. (2010). http://pmtksupport.googlecode.com/svn/trunk/GPstuff-2.0/dist/hammersley.m
38. Gablonsky, J.: Implementation of the DIRECT Algorithm. Center for Research in Scientific Computation, Technical Rept. CRSC-TR98-29, North Carolina State Univ., Raleigh, NC (1998)
39. Bichon, B.J., Eldred, M.S., Swiler, L.P., Mahadevan, S., McFarland, J.M.: Efficient global reliability analysis for nonlinear implicit performance functions. AIAA J. **46**, 2459–2468 (2008)
40. Echard, B., Gayton, N., Lemaire, M.: AK-MCS: an active learning reliability method combining Kriging and Monte Carlo simulation. Struct. Saf. **33**, 145–154 (2011)
41. Bect, J., Ginsbourger, D., Li, L., Picheny, V., Vazquez, E.: Sequential design of computer experiments for the estimation of a probability of failure. Stat. Comput. **22**, 773–793 (2012)

42. Balesdent, M., Morio, J., Marzat, J.: Kriging-based adaptive importance sampling algorithms for rare event estimation. Struct. Saf. **44**, 1–10 (2013)
43. Picheny, V., Ginsbourger, D., Roustant, O., Haftka, R.T., Kim, N.H.: Adaptive designs of experiments for accurate approximation of a target region. J. Mech. Des. **132**, 071008 (2010)
44. Dubourg, V., Sudret, B., Bourinet, J.M.: Reliability-based design optimization using Kriging surrogates and subset simulation. Struct. Multidiscip. Optim. **44**, 673–690 (2011)
45. Ranjan, P., Bingham, D., Michailidis, G.: Sequential experiment design for contour estimation from complex computer codes. Technometrics **50**, 527–541 (2008)
46. Jones, D., Schonlau, M., Welch, W.: Efficient global optimization of expensive black-box functions. J. Glob. Optim. **13**, 455–492 (1998)
47. Yang, X., Liu, Y., Gao, Y., Zhang, Y., Gao, Z.: An active learning Kriging model for hybrid reliability analysis with both random and interval variables. Struct. Multidisc. Optim. (accepted). doi:10.1007/s00158-014-1189-5
48. Matheron, G.: The intrinsic random functions and their applications. Adv. Appl. Probab. **5**, 439–468 (1973)
49. Dumas, A., Echard, B., Gayton, N., Rochat, O., Dantan, J.Y., Veen, S.V.D.: AK-ILS: an active learning method based on kriging for the inspection of large surfaces. Precis. Eng. **37**, 1–9 (2013)
50. Lophaven, S.N., Nielsen, H.B., Sondergaard, J.: DACE, a MATLAB Kriging toolbox, version 2.0. Tech. Rep. IMM-TR-2002-12; Technical University of Denmark (2002)
51. Luo, X., Li, X., Zhou, J., Cheng, T.: A Kriging-based hybrid optimization algorithm for slope reliability analysis. Struct. Saf. **34**, 401–406 (2012)
52. Kaymaz, I.: Application of kriging method to structural reliability problems. Struct. Saf. **27**, 133–151 (2005)
53. Jiang, C., Wang, B., Li, Z.R., Han, X., Yu, D.J.: An evidence-theory model considering dependence among parameters and its application in structural reliability analysis. Eng. Struct. **57**, 12–22 (2013)